RSC Advances

This is an *Accepted Manuscript*, which has been through the Royal Society of Chemistry peer review process and has been accepted for publication.

Accepted Manuscripts are published online shortly after acceptance, before technical editing, formatting and proof reading. Using this free service, authors can make their results available to the community, in citable form, before we publish the edited article. This *Accepted Manuscript* will be replaced by the edited, formatted and paginated article as soon as this is available.

You can find more information about *Accepted Manuscripts* in the Information for Authors.

Please note that technical editing may introduce minor changes to the text and/or graphics, which may alter content. The journal's standard Terms & Conditions and the Ethical guidelines still apply. In no event shall the Royal Society of Chemistry be held responsible for any errors or omissions in this *Accepted Manuscript* or any consequences arising from the use of any information it contains.

ROYAL SOCIETY OF CHEMISTRY

www.rsc.org/advances

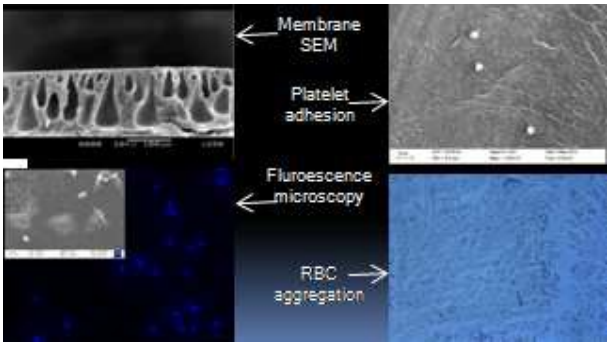

Three different formulations of dialysis grade membranes and their physiological, cyto and hemocompatibility have been presented.

RSC Advances Accepted Manuscript

In Vitro Cytocompatibility and Blood Compatibility for Polysulfone blend, surface modified polysulfone and Polyacrylonitrile membranes for hemodialysis

Anirban Roy[a], Prabhash Dadhich[b], Santanu Dhara[b], Sirshendu De[a,*]

[a]Department of Chemical Engineering, Indian Institute of Technology, Kharagpur P.O. Box 721302, India

[b]School of Medical Science and Technology, Indian Institute of Technology, Kharagpur P.O. Box 721302, India

* Corresponding author.

Tel: +91-3222-283926

Fax: +91-3222-255303

E-mail: sde@che.iitkgp.ernet.in

RSC Advances Accepted Manuscript

Abstract:

Fabrication of dialysis membranes with significant biocompatibility is an active area of research. In this context, three types of asymmetric flat sheet membranes were fabricated and compared for potential use as hemodialysis membranes. A polysulfone-polyvinylpyrrolidone and polyethylene glycol based polymer blend membrane; a polysulfone membrane surface modified by trimesoyl chloride and m-phenylene diamine and a polyacrylonitrile membrane were synthesized. All three types of membranes were characterized in terms of surface morphology, permeability, hydrophilicity, surface charge, porosity and mechanical strength. These were then subjected to comprehensive cytocompatibility and hemocompatibility tests as well as transport of uremic toxins. On basis of protein adsorption, oxidative stress, cell proliferation and adhesion, all three membranes were comparable. However, the blend and surface modified membranes showed excellent results for hemolysis, platelet adhesion, blood cell aggregation and degree of thrombus formation. All these results indicated the suitability of blend and surface modified membranes for possible dialysis application.

Keywords: Dialysis; polysulfone; polyacrylonitrile; cytocompatibility; hemocompatibility; uremic toxin transport.

1.0 Introduction

Dialysis in wake of kidney failure, or acute kidney injury (AKI) [1-3], is lifeline for survival of the patient. Replacing the kidney function with a membrane module in the extracorporeal circuit has resulted in shifting of focal point of nephrological research to development of biocompatible membranes. In past several decades, importance is given to polymeric material, blends and surface modifications to achieve better dialysis grade membranes with greater efficacy with improved biocompatibility. In this endeavour, cellulose actetate (CA) has been used since 1850's, following the pioneering work of Graham[4] and Fick[5], exhibiting its potential in ultrafiltration and dialysis. However, a whole gamut of

RSC Advances Accepted Manuscript

problems viz., low flux[6] and complement activation[7, 8], was encountered by practising clinicians with CA membranes. Ever since the program of Artifical Kidney-Chronic Uremia was launched by NIAMD (National Institute of Arthritis and Metabolic Diseases) in the year 1966, material scientists and engineers have started looking into the possibility of developing synthetic polymers for dialysis with significant hemocompatibility.

It led to the emergence of different materials with improved hemocompatibility. Therefore, polyacrylonitrile[9-11] (PAN) followed by polysulfone[12-14] (PSf) based membranes started to gain popularity in hemodialysis application. Polyethersulfone (PES) blended with citric acid grafted polyurethane[15] has been reported as possible dialysis membranes. Carbon nanotube grafted PES composite membranes[16], chemically modified PSf[17], vitamin E-TPGS composite membranes[18], as well as polyamide and monosodium glutamate blend membranes have also been explored for dialysis application[19,20]. However, biocompatibility was not the only issue for selection of membranes for practising clinicians. Development of high performance membrane has become pivotal issue in dialysis treatment, since higher and faster clearance of uremic toxins increases the patients' longevity[21, 22]. In fact, PSf based membranes have higher clearance rate of uremic toxins[23] and it has become a prime choice for clinicians administering dialysis, taking into account both its biocompatibility and transport properties[24].

In view of above discussion, it is clear that variants of PSf and PAN are suitable materials for hemodialysis application. Therefore, the present article is an attempt to formulate three types of dialysis grade membranes based on PSf and PAN and to evaluate their in vitro cell and blood compatibility as well as uremic toxin transport capabilities. The underlining step in synthesizing these membranes is attaining specified molecular weight cut off (MWCO) of around 6-16 kDa. Here, it was achieved in three different methodologies.

RSC Advances Accepted Manuscript

First, a polymer blend membrane (S1) was synthesized using polysulfone (PSf) as base material, blended with poly vinylpyrrolidone (PVP) and polyethylene glycol (PEG) of 6 kDa MWCO. Second, a PSf and PVP blend membrane (S2) was synthesized via surface treatment using trimesoyl chloride (TMC) and m-phenylene diamine (MPD) to yield similar cut off. Interestingly, TMC and MPD are in widespread use in synthesizing reverse osmosis membranes[25], but this has not yet been reported for its potential use as a dialysis membrane. Lastly, a polyacrylonitrile (PAN) homopolymer membrane (S3) was prepared of dialysis grade MWCO[26]. All membranes were characterized for permeability, hydrophilicity, porosity, membrane morphology and mechanical strength. Detailed cytocompatibility and hemocompatibility analysis were carried out to evaluate biological activity. Finally, performances of membranes were quantified in terms of their urea and creatinine permeances. The results were interpreted and a final recommendation was made in terms of performance. Therefore, novelty of this work includes formulation of PSf-PVP-PEG, surface modified PSf-PVP and PAN homopolymer membranes and exploring their suitability for hemodialysis purposes.

2.0 Materials and methods

2.1 Membrane synthesis

2.1.1 Polymer blend membrane

Polysulfone (average molecular weight 22,400 Da, supplied by M/s, Solvay Chemicals, Mumbai, India) 18 wt%, PVP (molecular weight 40,000 Da, supplied by M/s, Sigma Aldrich, Missouri, USA) 1, 2 and 3 wt% and PEG (supplied by M/s, S R Ltd, Mumbai, India) 3 wt% was dissolved in dimethyl formamide (DMF) (supplied by M/s, Merck (India) Mumbai Ltd.), by stirring over a magnetic stirrer (supplied by M/s, Anupam enterprises, Kharagpur, India) at around 60 $^{\circ}$C for over 10 hrs. The solution was then kept overnight for degassing and was cast the next day over a non-woven fabric support (118 ±

RSC Advances Accepted Manuscript

22.8 μm thickness supplied by M/s, Hollytex, India Inc., New York, USA). A film of thickness 150 μm was cast using a doctor's blade (fabricated and supplied by Gurpreet engg Works, Kanpur, India).

2.1.2 Polysulfone surface modified membrane

Polysulfone (18 wt%) and PVP (1 wt%) were dissolved in DMF with the help of stirrer as described in the previous section. The solution was kept overnight for degassing and was cast in the same manner as described in the previous section. The cast membrane was undergone surface treatment using TMC (supplied by M/s, Merck (India) Ltd.) and MPD (supplied by M/s, Merck (India) Ltd.). The membrane was first heated at 75 $^{\circ}$C for 10 min. Then it was immersed in 2% aqueous MPD solution for 5 min and air dried for 15 min. It was taken out and immersed in a 0.1% TMC solution (dissolved in hexane) for 5 min and then air exposed for 15 min. Finally, it was immersed in distilled water and left overnight.

2.1.3 Polyacrylonitrile (PAN) membrane

PAN supplied by M/s, Technorbital Advanced Materials Pvt. Ltd., Kanpur, India, was dissolved in DMF at around 60 $^{\circ}$C and was mechanically stirred (stirrer supplied by M/s, Anupam Enterprises, Kharagpur, India) for around 2 hours. Then, it was cast as described in the previous section.

2.2 Membrane characterization.

2.2.1 Permeability and MWCO

The MWCO and permeability of the cast membrane was found out using a stirred batch cell[27]. Firstly, the nascent membrane was compacted at 690 kPa for 3 hours and the permeate flux flow rate noted at five different transmembrane pressures[28]. The permeate flux was calculated by:

RSC Advances Accepted Manuscript

$$v_w = \frac{Q}{A\Delta T} \quad (1)$$

where, v_w is pure water flux; Q is volumetric flow rate of permeating water; A is effective filtration area (33.16 cm^2) and ΔT is sampling time. A plot of v_w against transmembrane pressure drop resulted in a straight line passing through the origin, the slope of which gave the hydraulic permeability of the membrane.

A wide range of Polyethylene glycol (PEG), comprising of various molecular weights, was supplied by M/s, S R Ltd, Mumbai, India. They were of molecular weights 1000, 4000, 10,000, 20,000, 70,000, 100,000 Da and are essentially neutral polymers. A 10 kg/m^3 solution, of each, was prepared by dissolving the polymers in distilled water separately and was fed to stirred batch cell[26]. Low transmembrane pressure (70 kPa) and high stirring speed (2000 rpm) was applied to minimize the concentration polarization layer, and the permeate was collected in intervals of five minutes and the percentage rejection (%R) was measured:

$$R = \left(1 - \frac{C_P}{C_F}\right) \times 100\% \quad (2)$$

where, C_P is concentration of permeate and C_F is concentration of feed. The rejection was calculated (Eq. 2) and plotted against the molecular weight of the solutes. The point of 90% rejection of solutes corresponds to the MWCO of the membrane.

2.2.2 Porosity

Porosity is measured by the difference in the wet weight and dry weight of the membrane. Membranes of specific dimensions were cut (2cm x 2cm) and immersed in distilled water and taken out after 5 min. The superficial water was dried off and their weights were measured (w_0). After this, they were placed in air circulating oven at 60^0C for

RSC Advances Accepted Manuscript

24 hrs and further dried in vacuum oven. Their dry weight (w_i) was then measured and porosity was calculated[29]:

$$\varepsilon = \frac{w_0 - w_i}{\rho_w A l} \times 100\% \quad (3)$$

where, ε is membrane porosity; A is the area of the membrane; l is membrane thickness and ρ_w is water density. The membrane porosity was measured three times and average values are reported.

2.2.2 Tensile strength

The mechanical strength of the membranes, as a function of yield stress was studied by a universal testing machine, procured from M/s, Tinius Olsen Ltd., Redhill, England of model H50KS. All the measurements were carried out at room temperature and at strain rate of 20 mm/min. The set of experiment consisted of three repetitions of each sample.

2.2.3 Contact angle

Contact angle was measured by a Goniometer (New Jersey, USA, Rame'-Hart, model No 200-F4) using the sessile drop method[30]. Contact angle at six different locations were measured and average value was reported.

2.2.4 Membrane morphology

The cast membranes were dried in a desiccators overnight and then were dipped in liquid nitrogen and fractured. They were gold coated and placed on stubs for the SEM images (model: ESM-5800, JEOL, Japan) at desired magnification.

2.2.4 Surface charge measurement

The surface charge of the three membranes was measured in an electroultrafiltration cell[31]. The operating conditions were: temperature = 298±2.0 K; transmembrane pressure = 0-2 bar; solution pH = 7.4; NaCl concentration = 0.01 M and cross flow velocity of 0.12 m/s. The streaming potential coefficient (V_P) was determined from the slope of the plot between

RSC Advances Accepted Manuscript

potential difference (ΔV) and pressure differential (ΔP) applied when the net current is zero. The relevant equations are:

$$V_P = \left(\frac{\Delta V}{\Delta P}\right)_{I=0} \quad (4)$$

$$\zeta = \frac{V_P \mu \lambda}{\varepsilon_0 D_i} \quad (5)$$

where, ζ is the membrane zeta potential, ε_0 is the permittivity in vacuum; D_i is the dielectric constant of the medium; μ and λ are the viscosity and conductivity of the feed solution.

2.3 Biological assessments of membrane

For *in vitro* biological assessment, NIH3T3 (Mouse embryonic fibroblast cell line) cells were procured from National Centre for Cell Science (NCCS) Pune, India. NIH3T3 cells were grown up to confluence in media containing alpha-modified essential media (αMEM) (12561-056, Invitrogen Life Sciences, India) with 1% antibiotics, antimyotic solution (penicillin 100µg/ml, streptomycin 10 µg/ml, and amphotericin-B 25 µg/ml; A002A Himedia, India) and 10% fetal bovine serum (Himedia, India) at 37^{o}C, 95% humidity and 5% CO_2 (Heracell150i, Thermo, USA).

For assessment of biological activity, membranes were cut into identical dimensions, sterilized and soaked in cell culture media for overnight. For each experiment, 1×10^4 cells/cm^2 were seeded on samples and control in a 12 well cell culture plate. Further, required volume of media was added to each well and cultured for particular time interval with respect to assay type. All the assays were performed in triplicate and their mean was reported. Commercially available dialysis fiber (Fresenius F6) was used as control in the experiment.

RSC Advances Accepted Manuscript

2.3.1 Metabolic activity

Preliminary cytocompatibility of prepared membranes was assessed to evaluate leaching of any toxic chemicals or any other adverse reaction to the cells by measuring metabolic activity through MTT (3-[4,5-dimethylthiazol-2-yl]-2,5 diphenyltetrazolium bromide) dye reduction assay on day three and seven according to previous report[32].

On respective day of assay, cell seeded membranes were rinsed with phosphate buffer saline (PBS), further incubated with 200 µl of 5mg/ml MTT solution (M5655, Sigma), in the dark, at standard cell culture condition. The dehydrogenase enzymes of metabolically active cells reduced the pale yellow MTT reagent to soluble purple colored formazan crystals. Formazan product was solubilised in dimethyl sulfoxide (DMSO) and absorbance was measured at 570 nm on microplate reader (Recorders and Medicare Systems, India). The absorbance was considered as proportional of living and growing cells.

2.3.2 Cell proliferation

DNA quantification assay on day three and seven was carried out to evaluate cell proliferation response of the seeded cells on membranes. After seeding, DNA content was measured using the DNA Quantitation Kit, Fluorescence Assay (DNAQF Sigma), according to the manufacturer's protocol. The double-stranded DNA binds primarily with fluorescent dye, bisBenzimide H 33258 (Hoechst 33258), which were measured fluorometrically at an excitation wavelength of 350 nm and an emission wavelength of 460 nm. Standard DNA concentration curve was plotted with standard solution of calf thymus DNA (D4810 Sigma).

2.3.3 Oxidative stress analysis

Cell sample interaction may enhance intercellular reactive oxygen species (ROS) production, which affects cellular microenvironment. Therefore, release of ROS measured

RSC Advances Accepted Manuscript

quantitatively via Di-Chloro Di-Hydrofuran Fluorescein Di-Aceteate (DCFH-DA) assay according to previously mentioned report[33]. Cell seeded well with samples were rinsed with PBS and incubated with 1 mM methanolic DCFH-DA solution (Sigma-Aldrich) at 37 ^{o}C for 1 h. Further, fluorescence intensity of cell interacted DCFH-DA was measured by excitation at 485 nm and emission at 530 nm on fluorescence spectrometer (Perkin Elmer, UK).

2.3.4 Estimation of total protein content

Protein adsorption is an important parameter for evaluating biological response towards dialysis membrane application. Protein adsorption was measured by two different methods. In each method, equal size (2 cm^2 surface area) of membrane samples was used.

2.3.4.1 Indirect Method: NIH3T3 cells were seeded on membranes for day three and five. Total protein concentration of cell cultured samples was quantified by bicinchoninic acid (BCA) protein assay[34]. Briefly, PBS rinsed cell seeded samples were incubated with BCA working solution (50 parts of BCA reagent with one part of 4% copper sulfate pentahydrate, green colored solution) at 37 ^{o}C for 30 min. During the incubation, free amino acid got reduced and formed crimson colored complex with BCA. Concentration of this colored complex concentration was assessed by absorbance at 562 nm on microplate reader (Recorders and Medicare Systems, India). Standard protein concentration curve was plotted with known concentration of bovine serum albumin.

2.3.4.2. Direct Method: Membranes were incubated in phosphate buffer solution (0.02M, pH 7.4) containing bovine serum albumin (BSA, 5 g/dl), human γ-globulin (1.5 g/dl) and human fibrinogen (0.45 g/dl) at 37 ^{o}C for 2 hours. Further, samples were gently rinsed with PBS three times. Samples were kept in 1 wt% aqueous solution of sodium dodecyl sulfate (SDS)

RSC Advances Accepted Manuscript

for 60 min at room temperature on a shaker. Adsorbed proteins were removed from samples and measured by bicinchoninic acid (BCA) protein assay[34].

2.3.5 Cell attachment and morphology

Cell attachment and morphology of NIH3T3 cells were evaluated by scanning electron microscope and fluorescent microscope on day three and seven[35]. For SEM analysis, cell seeded film samples were rinsed gently by PBS, fixed by 4 % para formaldehyde at 37 ^{o}C, further dehydrated with gradient ethanol solution and vacuum dried for overnight. Prior to SEM microscopy, samples were gold coated (Polaron, UK).

For fluorescent imaging, cell seeded membranes were washed thrice with PBS and cells were fixed with 4% paraformaldehyde followed by permeabilization of cells using cell lysis solution (0.1% triton X in PBS). Cells fixed on film were stained with hoechst dye (H1399, InvitrogenLife Sciences) according to manufacturer's instructions. Images were acquired with Axio Observer Z1(Carl Zeiss, Germany).

2.4 Hemocompatibility test

Hemocompatibility analysis of prepared membranes is an essential requisite towards dialysis membrane application. For hemocompatibility assay, whole blood was collected from healthy donors in polyethylene disposable syringe containing 4.9 % citrate-phosphate-dextrose-adenine (CPDA) solution. The blood was mixed well with anticoagulant solution and following tests were performed as presented in subsections. Commercial available fiber as control was not included or compared in hemocompatibility studies due to difficulty to obtained active (inner) surface of blood contact. Sample size was kept similar in each test and equilibrated with normal saline via incubation for one hour before each test. All the assays were performed in triplicate and their mean was reported.

RSC Advances Accepted Manuscript

2.4.1 Hemolysis assay

Hemolysis assay was carried out to evaluate RBC compatibility of samples. Normal saline equilibrated samples were kept with freshly collected uncoagulated blood. Further, incubated for 1 hour at 37^{o}C, 95% humidityand5%CO_2 (Heracell150i, Thermo, USA). Subsequently, RBC lytic activity was quantified through measuring optical density at 540 nm. Normal Saline and 1% Triton-X solution were used as positive and negative controls as well.

2.4.2 Blood Cell Aggregation

To ascertain changes in surface property of blood cells, blood cell aggregation study was conducted. Blood cell aggregation was carried out by modification of previously reported method[2]. For RBC aggregation study, freshly collected blood was centrifuged at 700 rpm. Collected pellet was resuspended with normal saline in 1:9 volume ratio. Further, 100 µL of this solution was mixed with 600 µL of normal saline. Equal sizes of membranes were incubated with prepared suspension for 1 hour at 37 ^{o}C. For WBC aggregation study, WBC was isolated from uncoagulated freshly isolated blood by ficoll paque mononuclear cell isolation principle using HiSep^{TM} LSM-1077 (Himedia) with manufacturer's instructions. Isolated WBC were mixed with normal saline and incubated with membranes as previously. After incubation, the cell suspension was smeared on a glass slide and observed under microscope (Axio Observer Z1Carl Zeiss, Germany).

2.4.3 Platelet adhesion

Fresh blood with anticoagulant was centrifuged at 1500 rpm to collect platelet rich plasma (PRP). Normal saline pre-equilibrated samples were incubated with PRP blood for 2 hour at 37^{o}C, 95% humidity and 5% CO_2 (Heracell150i, Thermo, USA). After incubation,

RSC Advances Accepted Manuscript

samples were rinsed gently with normal saline, fixed by 4 % para formaldehyde at 37 ^{o}C, further dehydrated with gradient ethanol solution and vacuum dried for overnight. Before optical characterization under SEM, samples were gold coated (polaron, UK).

2.4.4 Thrombus formation

Normal saline equilibrated samples were incubated with freshly collected whole human blood in a 24 well plate for 2 hour at 37^{o}C, 95% humidity and 5% CO_2 (Heracell150i, Thermo, USA). Further, samples were rinsed thrice gently with normal saline, fixed by 4 % para formaldehyde at 37 ^{o}C, further dehydrated with gradient ethanol solution and vacuum dried for overnight. The degree of thrombosis (DOT) was measured with described method[36] as follows:

$$DOT = \frac{W_t - W_d}{W_d} \quad (6)$$

where, W_t is the weight of blood treated sample and W_d is weight of dry weight of sample before blood treatment.

2.5 Urea and creatinine transport

The cast membranes were tested in terms of their urea and creatinine permeances. The set up is described in Fig. 1. Flat sheet membranes, which were cast as described in the previous sections, were cut to fit into the cross flow membrane module. The peristaltic pump drives the feed fluid from the feed tank through the rotameter into the membrane module. The dialysate side fluid is pumped from the dialysate tank by the peristaltic pump through the rotameter into the membrane module. The urea and creatinine permeate through the membrane from the feed to the dialysate side flowing in a cross flow pattern. The flow rate of the feed side was maintained at 250 ml/min and that of the dialysate side was 250 and 500

RSC Advances Accepted Manuscript

ml/min. Concentration of urea and creatinine in the feed was 500 mg/l and 20 mg/l, respectively.

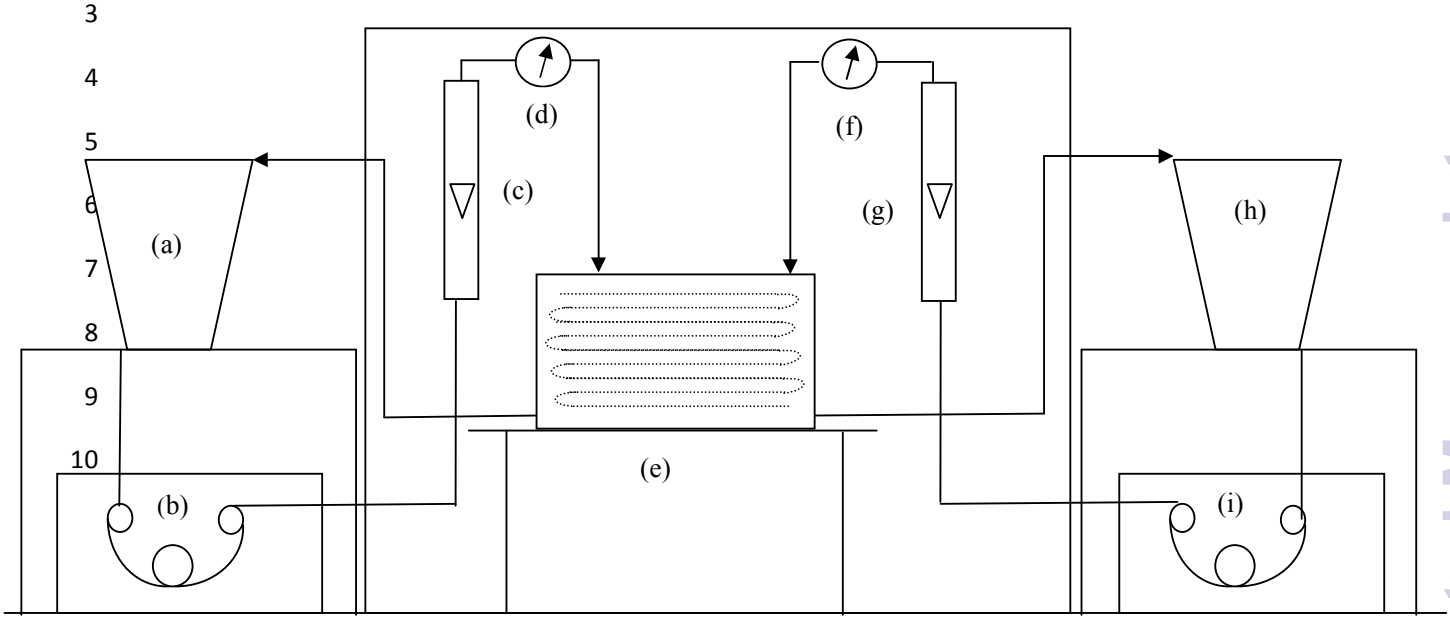

Fig. 1: Experimental set up for measuring urea and creatinine permeances: (a) Feed tank; (b) Peristaltic pump; (c) Rotameter; (d) Pressure gauge (sphygmomanometer); (e) Cross flow membrane module; (f) Pressure gauge (sphygmomanometer); (g) Rotameter; (h) Dialysate tank; (i) Peristaltic pump.

2.6 Statistical analysis

All the experiments were carried out in triplicate. Two-tailed Student's t-test was carried out for all the data sets and expressed as a mean ± standard deviation (SD). Differences were considered to be significant at $p < 0.05$. The SD value of each measurement is presented in different figures.

RSC Advances Accepted Manuscript

3.0 Results and discussion

3.1.1 Permeability, MWCO and contact angle

The permeability and contact angle are represented in Fig.2 for the three membranes. It is evident from this figure that PAN (S3) is most hydrophobic membrane with highest contact angle of 80 °. This higher degree of hydrophobicity is linked to depleted hydrogen-bond interaction sites with water. Due to this, hydrophobic solutes experience a spontaneous adsorption on the membrane[37], resulting in fouling of the membrane surface. However, in case of dialysis, this problem of protein adsorption leads to bigger complication, like complement activation. This phenomenon also results in lower flux. S3 membrane has a permeability of around 0.2×10^{-10} m/s.Pa, which is the least of the three membranes. The surface modified membrane (S2) has a higher contact angle than S1 but lower than S3. This can be attributed to the fact that adding PVP to PSf induces hydrophilicity which decreases the contact angle to 73 °. Contact angle of S1 is 69 º, lowest of the three membranes, since it has two hydrophilic polymers in the blend, viz, PVP and PEG. This nature of hydrophilicity is reflected in the results of permeability as well. The permeability of S2 is 0.6×10^{-10} m/s.Pa, and that for S1 is 1.4×10^{-10} m/s.Pa. The MWCO of all the membranes is 6 kDa, as presented in Fig. 2(b).

RSC Advances Accepted Manuscript

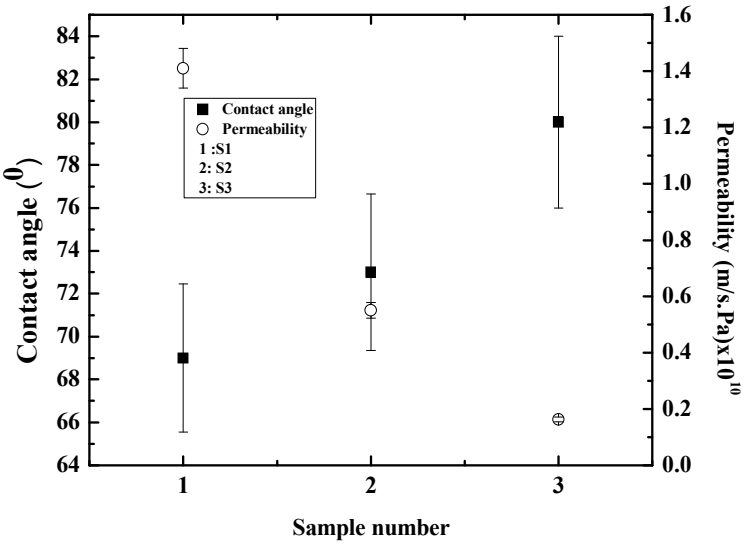

Fig.2(a) : Permeability and contact angle of the three membranes.

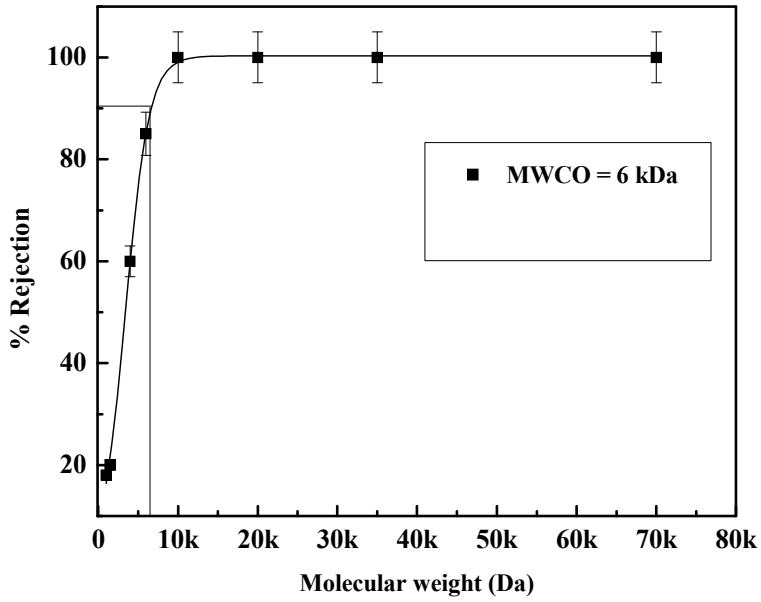

Fig.2(b) : MWCO of S1, S2 and S3 membranes.

RSC Advances Accepted Manuscript

3.1.2 Porosity, surface morphology and tensile strength

The cross section images show the typical formation of phase inversion membrane, i.e., a thin skin followed by a porous sub structure, and a spongy bottom layer. Surface morphology can be attributed to the addition of hydrophilic polymers to the blend. During phase inversion, addition of hydrophilic polymers induces more water flux into the membrane structure, thereby increasing the number of macrovoids. This is reflected in the SEM images (Fig.3) S1 has a more porous structure than S2 and S3. However, the skin thicknesses of all the three membranes are almost same and this shows that even though the porous nature of the membranes varies, the MWCO of the membranes being the same, the skin thickness of the membranes is comparable. The porosity and tensile strength is represented in Fig.4. It is evident from the above discussion that the porosity of the membranes increase in order of S3<S2<S1. While, S3 has a porosity of 54%, that of S1 has porosity of 62%. S2 has an intermediate porosity of 60%. The porosity has an exact mirror reflection in the breaking stress relationship. It follows the similar trend, i.e., increase in extent of porosity reduces mechanical strength and thus reduction in breaking stress. Hence, the failure stress of S1, S2 and S3 membranes are 6 MPa, 7 MPa and 11 MPa, respectively.

RSC Advances Accepted Manuscript

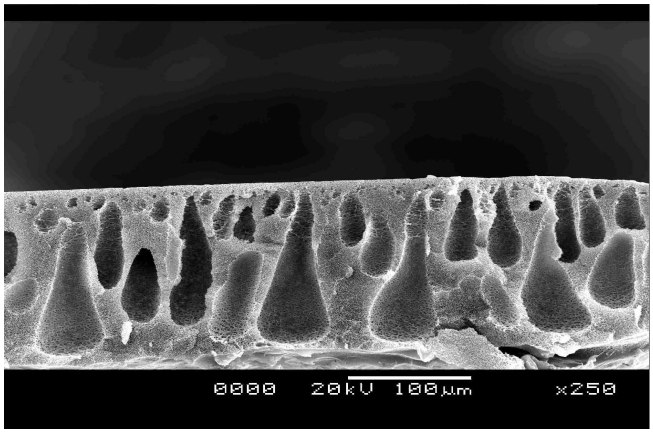

1

(a)

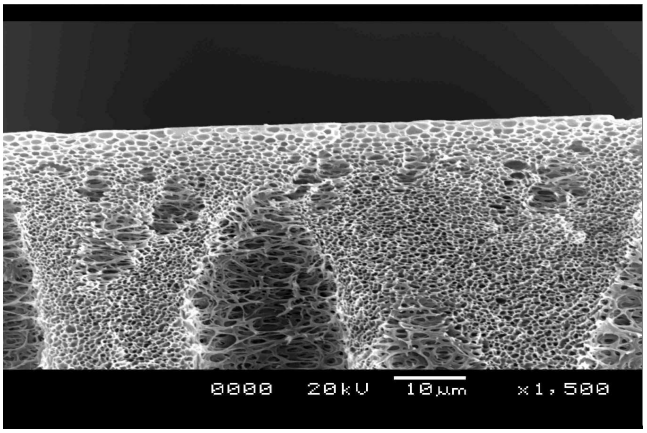

(d)

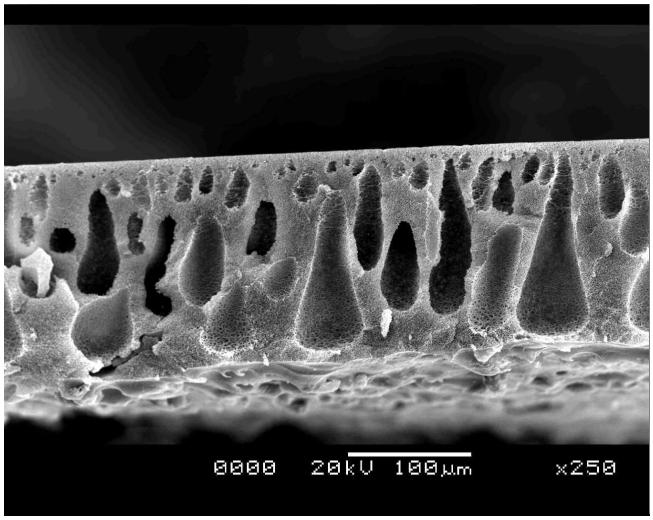

2

(b)

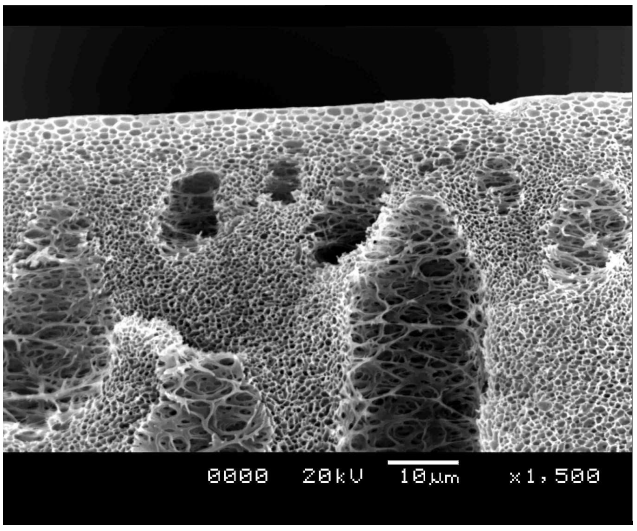

(e)

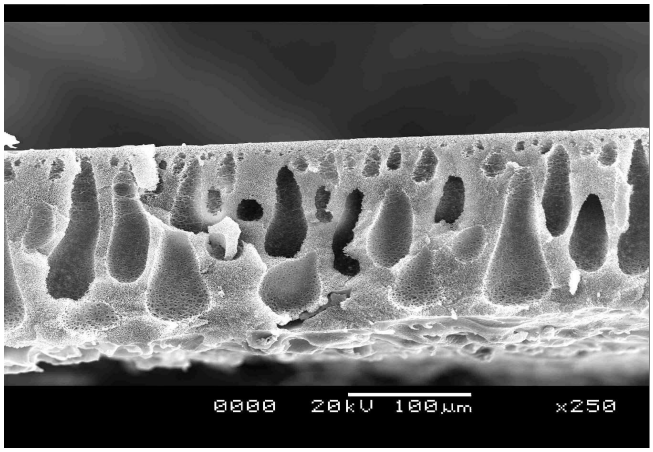

3

(c)

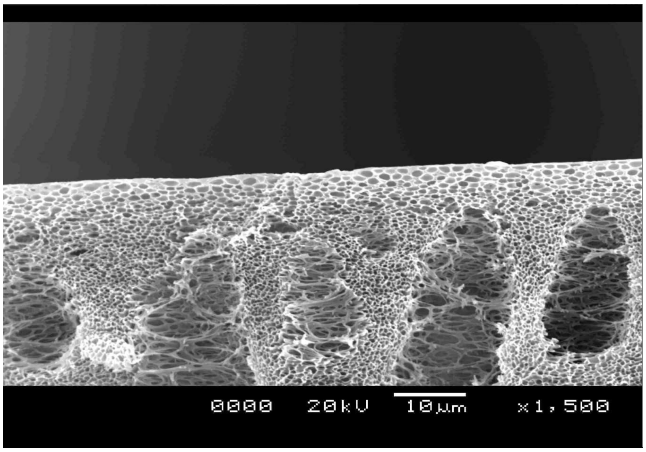

(f)

4

Fig. 3: SEM images of the three membranes: (a) Cross section of S1; (b) Cross section of the S2; (c) Cross section of S3; (d) Skin image of S1; (e) Skin image of S2; (e) Skin thickness of S3.

RSC Advances Accepted Manuscript

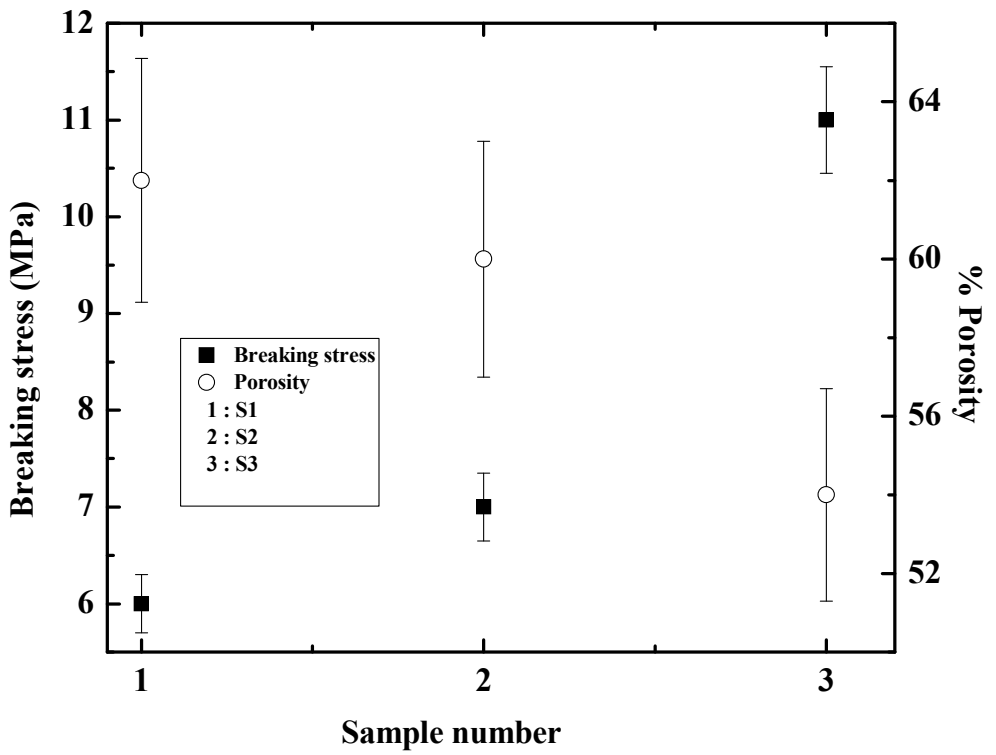

Fig. 4: Breaking stress and porosity for the three membranes.

3.1.3 Surface charge measurement

The surface charge of three membranes were determined at neutral pH and it was found that S1 and S2 were nearly neutral (0.0 to 0.1 mV). S3 was slightly negative in charge (-0.03 mV) which can be attributed to presence of nitrile groups.

3.2 Biological assessments of membrane

3.2.1 Metabolic activity and Cell proliferation

Cytocompatibility of dialysis membrane is an important parameter owing to its application towards plasmapheresis, hemodialysis, hemodiafiltration and related blood and body fluid purification. In this context, NIH3T3 cell metabolic activity was evaluated through MTT assay on day three, five and results are displayed in Fig.5. The synthesized formazan

RSC Advances Accepted Manuscript

absorbance of prepared membranes are higher compared to control (0.48 ± 0.01 and 0.80 ± 0.01 on day three and five), demonstrating satisfactory cytocompatibility. Notably, S2 and S3 displayed similar growth kinetics as 0.50±0.03, 0.56±0.03 on day three and 0.83±0.04, 0.88±0.04 on day five, where S1 displayed higher cell metabolic activity as 0.67 ± 0.05 and 1.06 ± 0.05 on day three and five, respectively. Therefore, it can be concluded that all three membranes qualified cytocompatibility and have favourable biological activity.

These results further confirmed with cell proliferation analysis. The cell proliferation activity of the seeded cells was measured by DNA quantification assay as summarized in Fig.6. It displayed similar growth pattern as MTT assay. The cell proliferation rate of all three membranes was significantly higher as compared to control (41.82 ± 0.1, 63.94 ± 0.2 on day three and five, respectively). The absorbance value for S1 seeded cells was 49.4 ± 0.3 on day three of cell seeding followed by 78.08± 0.1 on day five; however DNA bound dye absorbance values for seeded cells on S2 and S3 were 41.16 ± 0.7, 43.59 ± 0.2 on third and 60.46 ± 0.3, 67.15 ± 0.2 on fifth day, respectively. Here similar to metabolic activity, S1 displayed higher cell proliferation rate, subsequently higher cell viability, which is expected due to the fact that PSf-PVP membranes are reported to be biocompatible[38]. Interestingly, S2, being a surface modified membrane, too exhibited comparable biocompatibility. This fact is further corroborated in sections discussed below.

RSC Advances Accepted Manuscript

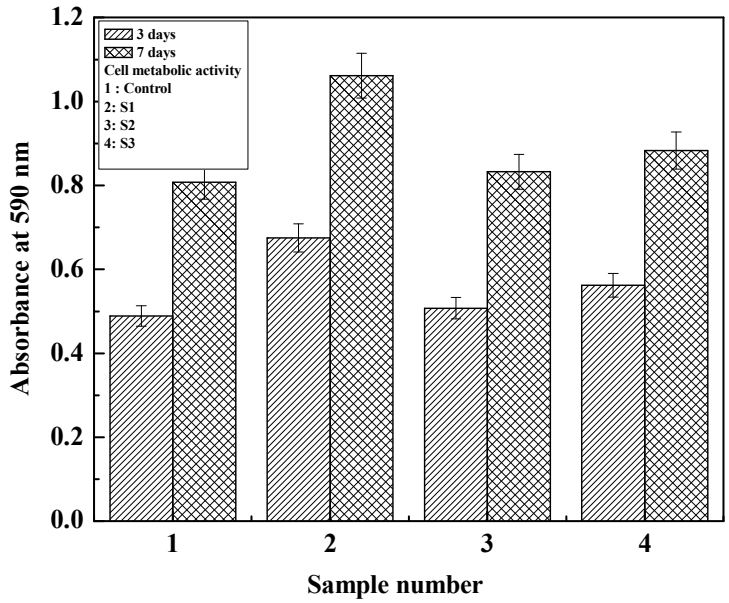

Fig.5: Cell metabolic activity of the three membranes

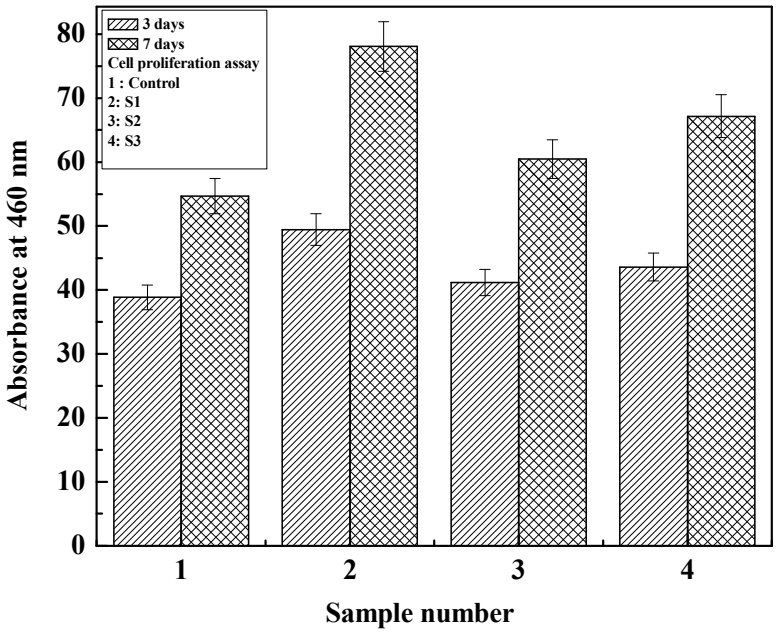

Fig.6: Cell proliferation assay of the three membranes.

RSC Advances Accepted Manuscript

3.2.2 Oxidative stress analysis

Cell cytocompatibility further verified by measuring oxidative stress on seeded cells in presence of membrane samples. Previously described Di-Chloro Di-HydrofuranFluorescein Di-Aceteate (DCFH-DA) assay was used to quantify reactive oxygen species (ROS). During incubation with seeded cells, DCFH-DA used to get oxidized and form fluorescent active 20, 70-dichlorofluorescein (DCF). The concentration of DCF directly proportional to newly formed ROS, finally measured as fluorescent intensity as displayed in Fig.7. The DCF fluorescent intensity was found increasing with duration. Interestingly, control sample displayed highest ROS activity among all sample on day three. S2 and S3 initially displayed lower ROS activity but it enhanced and similar to control with duration of incubation. S1 has displayed lower activity compared to control on day three and five as well. This can be attributed to the general cytocompatibility exhibited by PSf-PVP blend membranes. However, S2 exhibited comparable results. It may be owing to phenylenediamine. Phenylenediamine derivatives have well reported antioxidant activity[39] due to primarily three mechanisms: (i) free-radical scavenger ability[40], (ii) inhibition of oxidative glutamate toxicity and (iii) acting as peroxide decomposers by the eliminating oxidative catalyst to avoid further oxidation[41].

RSC Advances Accepted Manuscript

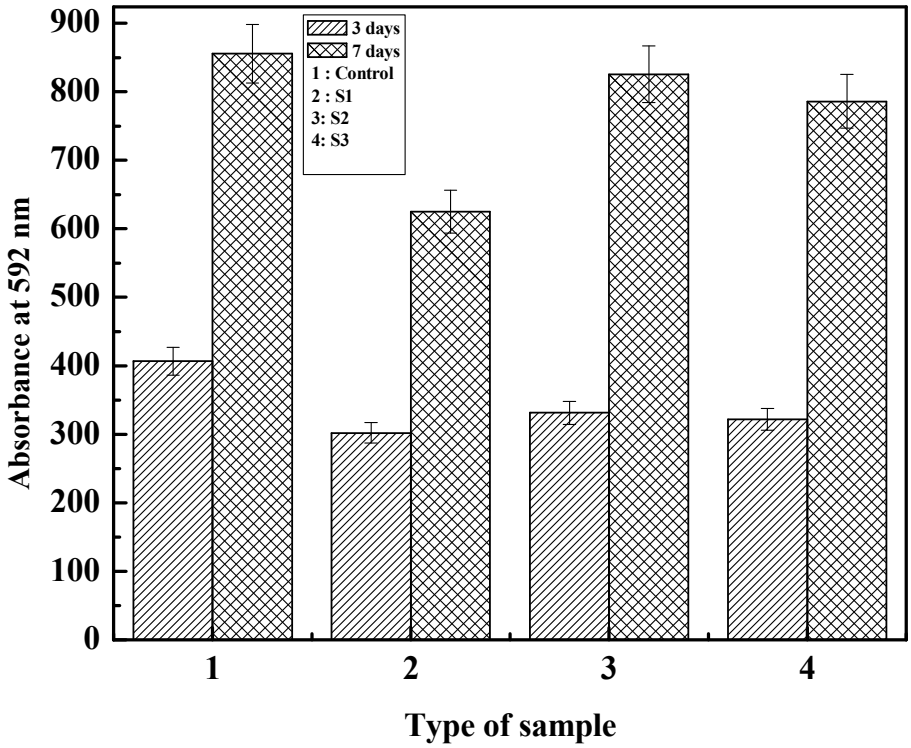

Fig. 7: Oxidative stress of the three membranes.

3.2.3 Estimation of total protein content

Protein adsorption study of prepared membranes is prerequisite towards blood dialysis application. It has been reported that adsorption of plasma proteins is one of the key issues to evaluate hemocompatibility of respective material. Here protein adsorption was measured through direct (using human plasma proteins such as albumin, γ-globulin and fibrinogen) and indirect methods (via NIH3T3 cell incubation).

According to earlier studies, proteins preferably are adsorbed on hydrophobic surfaces. In an aqueous system, initial surface hydration of hydrophobic material governs the subsequent protein adsorption[9]. In this direction, hydrated protein molecules displace the

RSC Advances Accepted Manuscript

interfacial water through electrostatic interaction to achieve thermodynamic equilibrium[42, 43]. Therefore, the prepared sample is supposed to have good protein adsorption properties owing to near hydrophobic nature. In direct method, the protein adsorption behavior of sample membranes incubated with predefined human plasma protein solution is displayed in Fig.8. Control sample displayed very high protein absorption properties (0.04 ± 0.001). S3 being the most hydrophobic membrane (contact angle 80^{o}) among all prepared membranes exhibited higher protein adsorption. Similar results were obtained for both S2 (contact angle 73^{o}) and S1 (contact angle 69^{o}) having less hydrophobic nature. S1 displayed lowest protein adsorption property (0.008 ± 0.0005) compare to S2 (0.013 ± 0.001) and S3 (0.019 ± 0.002).

Here, it has to be noted that the surface charges, albeit present, are marginal in magnitude. Hence, surface hydrophilicity/hydrophobicity is the dominant factor influencing protein adsorption in such cases[44, 45]. Hydrophilicity helps forming a thin layer of aqueous film on the surface of the membrane, impeding the advance and deposition of the proteins on the membrane surface leading to less adsoption of protein. Hence, S1 and S2 experience lower protein adsorption than S3. Moreoever, zwitter-ionic/mixed-charge hydration phenomena does not exist over here owing to high contact angle (73^{o}) compared to zwitter-ionic surfaces (<20°). During indirect protein adsorption study, similar results were obtained. S1 displayed lowest protein adsorption profile compare to S2 and S3.

RSC Advances Accepted Manuscript

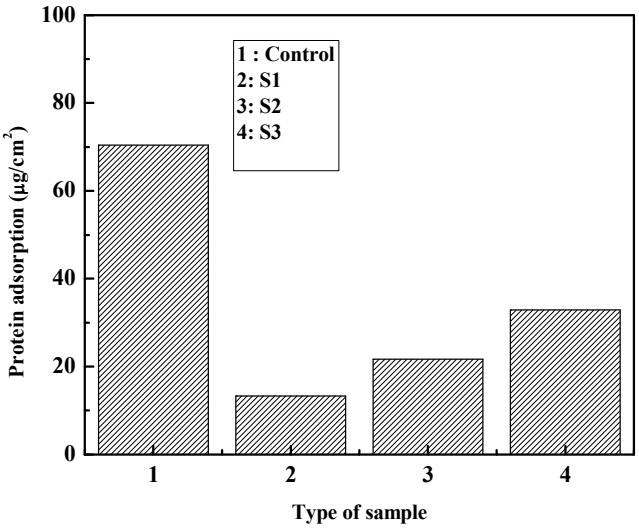

Fig. 8: Total protein adsorption.

3.2.4 Cell attachment and morphology

Cell attachment and proliferation on membranes were evaluated through seeding cells for three and seven days. Cell seeded membranes were observed under SEM and fluorescent microscope as displayed in Fig.9. The membranes displayed very less cell attachment initially on day three, further few cells were observed on S2 and S3 on day seven. As reported in literature[46], surface characteristic, such as surface charge, surface roughness, hydrophilicity, play an important role in improving the membrane performance for hemodialysis applications. In this context, hydrophilicity imparts a thin film of water near the surface of the membrane thereby decreasing the interactions between the proteins and also prevents cell adsorption. S1 membranes do not show any cell attachment due to higher hydrophilicity, near neutral surface charge and highly smooth surface. Commercial available fiber as control was not included in this study due to difficulty of obtaining active (inner) surface of blood contact.

RSC Advances Accepted Manuscript

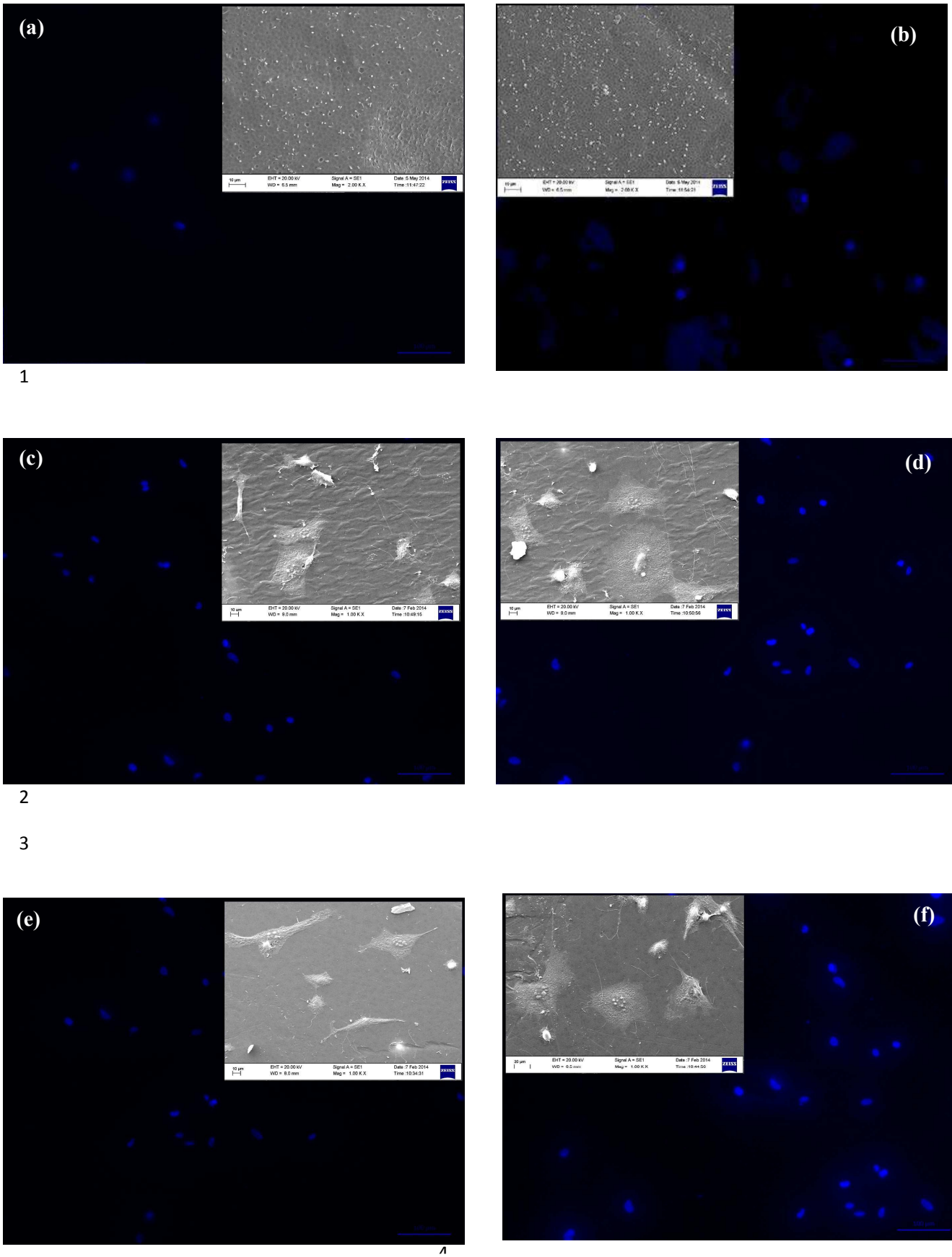

Fig. 9: Cell attachment and morphology study (Inset – SEM; Main - Fluorescent): (a) S1, 3 days, (b) S1, 7 days, (c) S2, 3 days, (d) S2, 7 days, (e) S3, 3 days, (f) S3, 7 days.

RSC Advances Accepted Manuscript

3.3 Hemocompatibility test

3.3.1 Hemolysis assay

For hemodialysis applicability, the membranes were incubated with fresh blood to test RBC hemolysis and result is reported in Fig.10. It was observed that up to 2 hour, there was no significant change in hemolysis. All the samples were found comparable with positive control, causing less than 2% hemolysis which suggests blood cell compatibility of the membranes. The hemolytic behaviour is further substantiated with blood cell aggregation assay as discussed in the succeeding section.

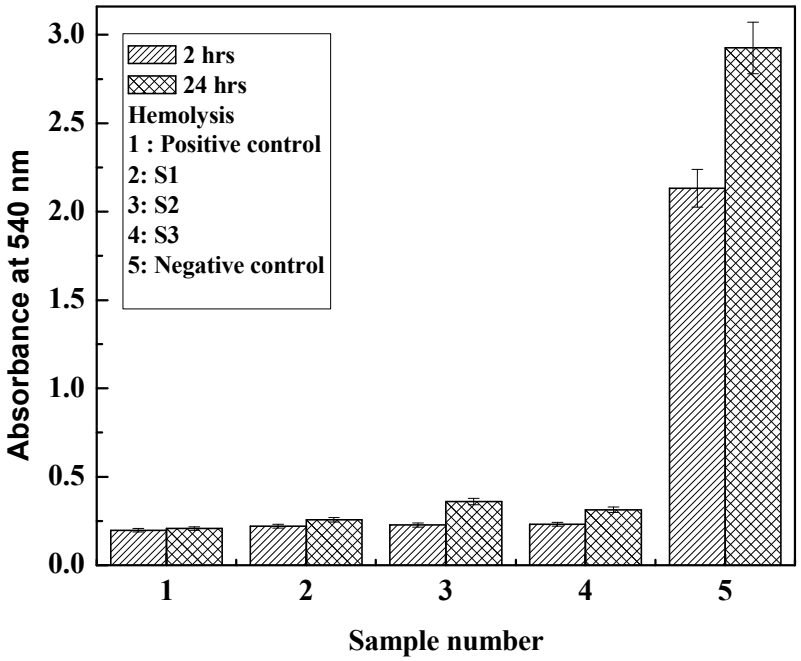

Fig. 10: Hemolysis assay of the membranes.

RSC Advances Accepted Manuscript

3.3.2 Blood Cell Aggregation

Blood cell aggregation test was performed to ensure hemocompatibility of membranes and the results are presented in Fig.11. There was no significant RBC aggregation observed in all the membranes. Few WBC were found ruptured in S3, without significant WBC aggregation behavior in any of the membranes. These further support the hemolysis assay results (discussed in 3.3.1) towards hemocompatibility of the membranes.

It has been reported that antifouling properties, surface charge and smoothness control blood cell compatibility and aggregation activity during hemodialysis[46]. The promising blood cell compatibility activity of S1 membranes is due to the incorporation of PVP, which is enhancing the hydrophilicity of membrane, resulting in reduced adsorption of proteins. Further, blending with PSf-PEG causes reduced oxidative stress and limits the surface charge to near neutral, which is also in agreement with reported literature[47]. Similar reasons are attributed towards comparable blood cell compatibility of S2 membrane. Additionally, phenylenediamine reduces the ROS activity as discussed previously. S3 also has similar hemolytic activity, but reduced hydrophilicity and negative surface charge leading to cell aggregation

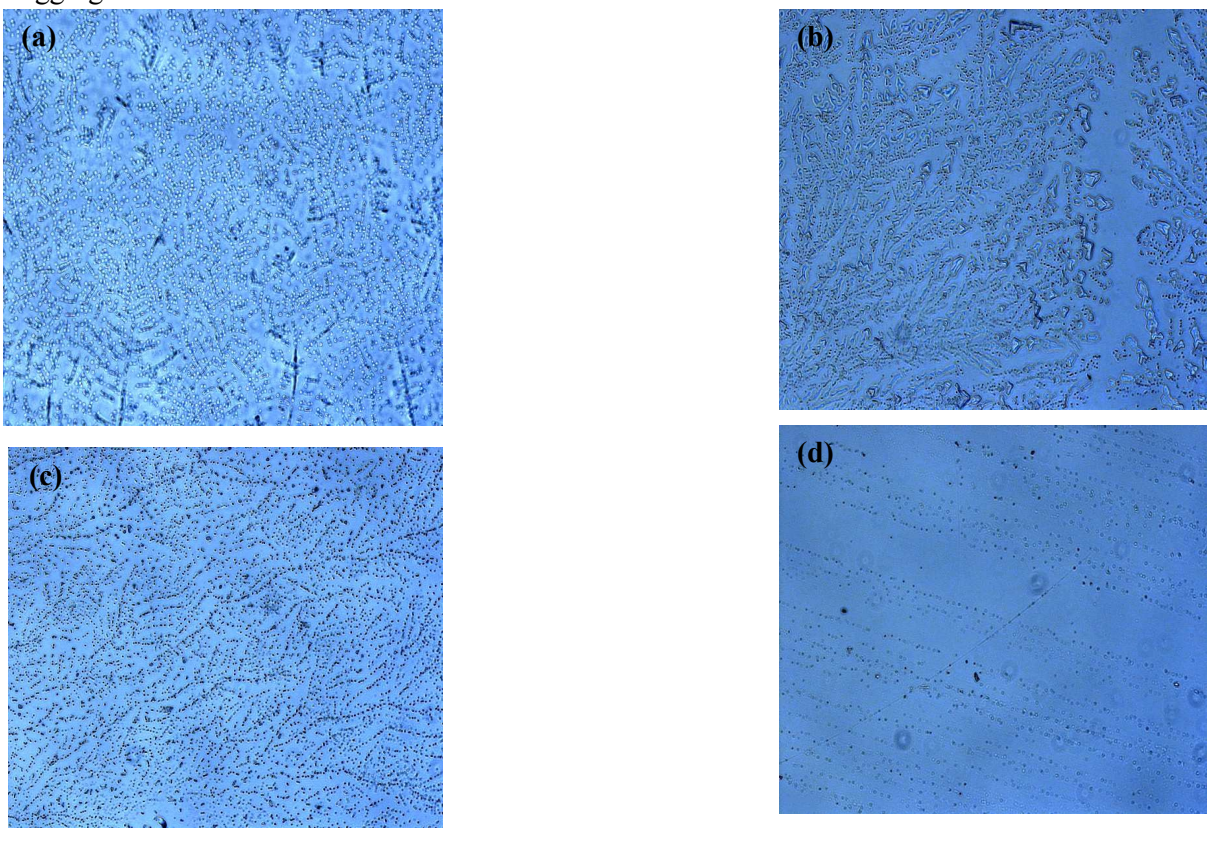

Fig. 11 : RBC aggregation on the three membranes; (a) Control; (b) S1; (c) S2; (d) S3.

RSC Advances Accepted Manuscript

3.3.3 Platelet adhesion

The protein adsorption, platelet adhesion and activation on the membranes are closely interrelated phenomena. SEM micrograph of PRP incubated membranes displayed in Fig.12. It has been observed that maximum number of platelets were adhered and aggregated on S3 membranes. S2 exhibited comparatively lower platelet adhesion to S3 without any morphological changes and aggregation as found in S3. The platelet adhesion on S1 membranes was significantly less compare to S2 and S3.

The lower platelet adhesion on S1 is believed to be dependent on protein adsorption behaviour. According to Ishihara et al. (1999) fibrinogen adsorption is prerequisite for platelet adhesion[48]. The neutral surface charge results in repulsion of protein and negatively charged platelet. Tanaka et al. (2000) observed that beside fibrinogen adsorption, its conformation also needs to be changed towards platelet adhesion[49]. Adsorbed fibrinogen with native conformation structure never participates in platelet adhesion and activation. In this context, S2 sample has lower fibrinogen adsorption without significant conformation changes compared to S3, resulted in low platelet adhesion and non-aggregation.

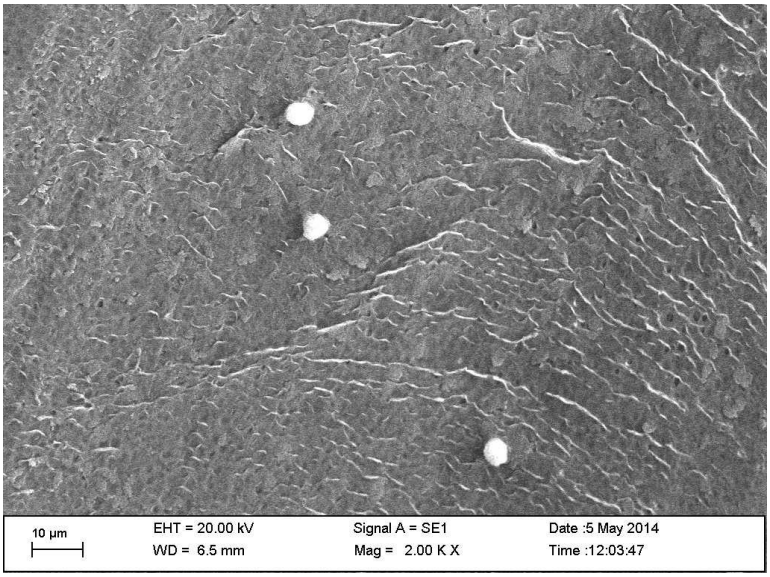

(a)

RSC Advances Accepted Manuscript

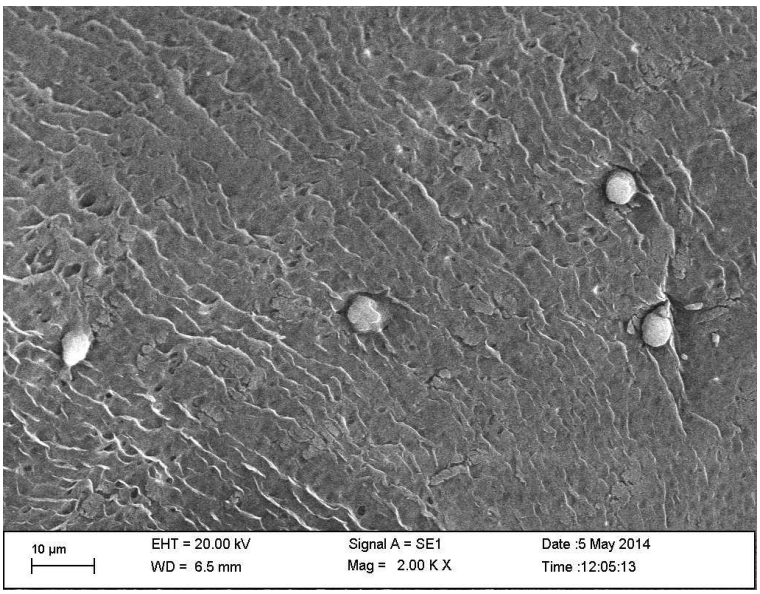

(b)

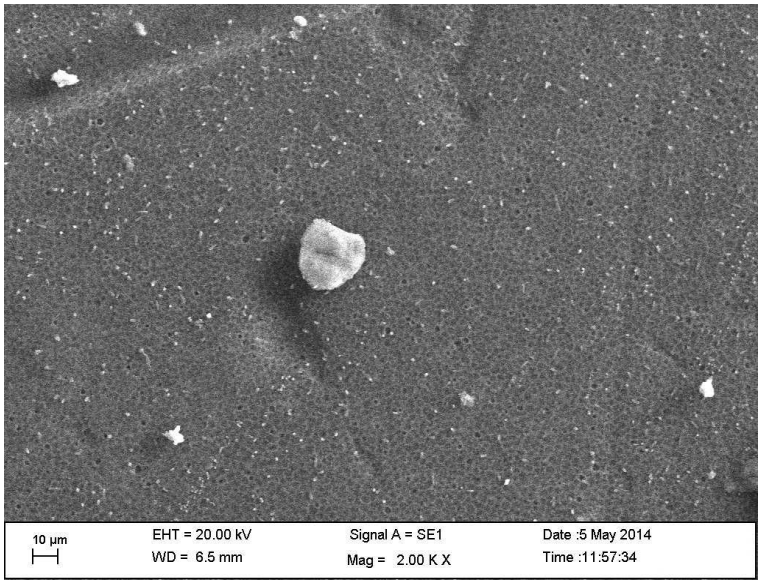

(c)

Fig. 12: Platelet adhesion on the three membranes: (a) S1, (b) S2, (c) S3.

3.3.4 Thrombus formation

The thrombus formation properties were evaluated for all three prepared membranes. The outcome is in line with the results obtained in the previous platelet adhesion and protein adsorption. Therefore, significant difference in thrombus formation behaviour was observed

RSC Advances Accepted Manuscript

among the three membranes. Fig.13 displays the thrombus formation behavior of different membranes. S1 and S2 exhibit similar thrombus formation activity. S3 membrane shows the highest degree of thrombus (DOT) as 0.63 compared to S1 and S2 0.31 and 0.37, respectively.

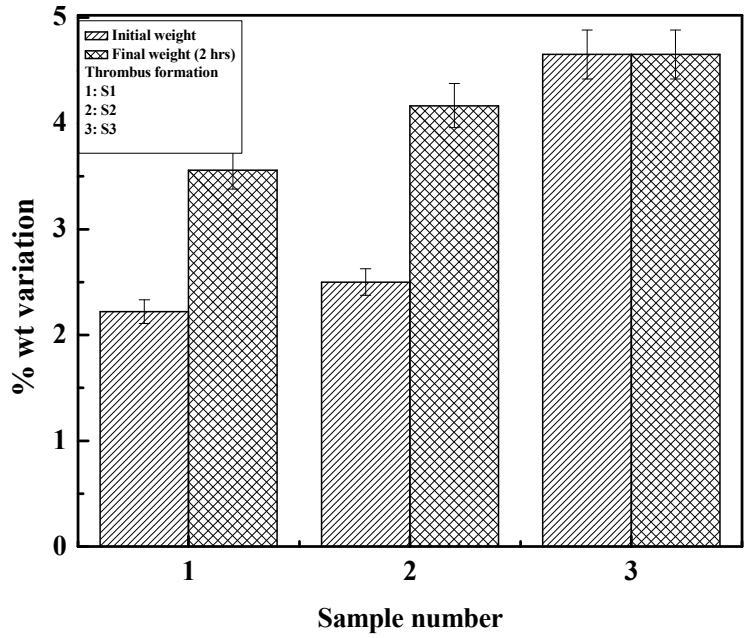

Fig. 13: Thrombus formation on the three membranes.

3.4 Urea and creatinine permeation

The urea and creatinine transport through the membranes are depicted in Fig.14. It is evident from the figure that S1 has the highest uremic toxin transport rate than S2 or S3. While the time taken for S1 and S2 to bring down the urea concentration in feed tank to the desired levels (400mg/l), is around 120 minutes, the same for S3 is 180 minutes. Similarly, the creatinine transport requires 120 minutes for S1 to bring down the concentration to 12 mg/l. However, the rates are much slower for S2 and S3. This can be explained on the basis

RSC Advances Accepted Manuscript

of the permeability behaviour of the three membranes (section 3.1.1). While the permeability of S1 is highest, that of S3 is lowest. Given the same MWCO of the three membranes, this would automatically imply that transport rate of the solutes would decrease as permeability decreases.

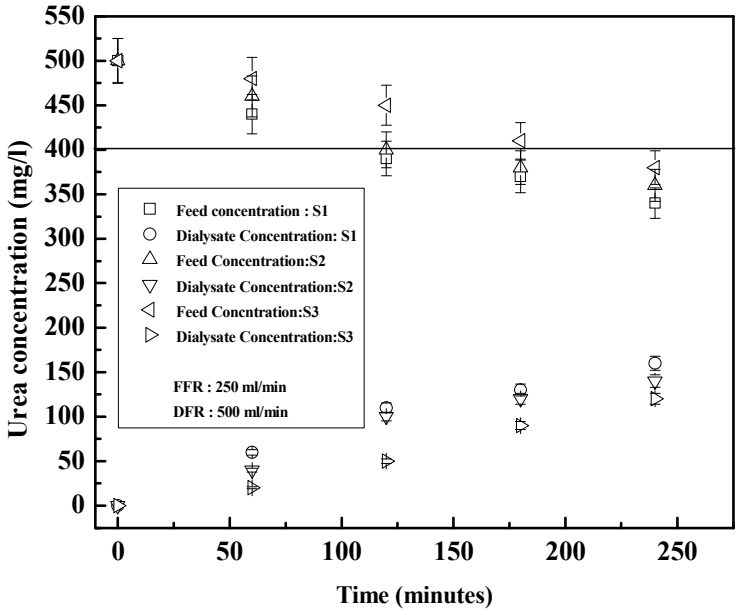

(a)

RSC Advances Accepted Manuscript

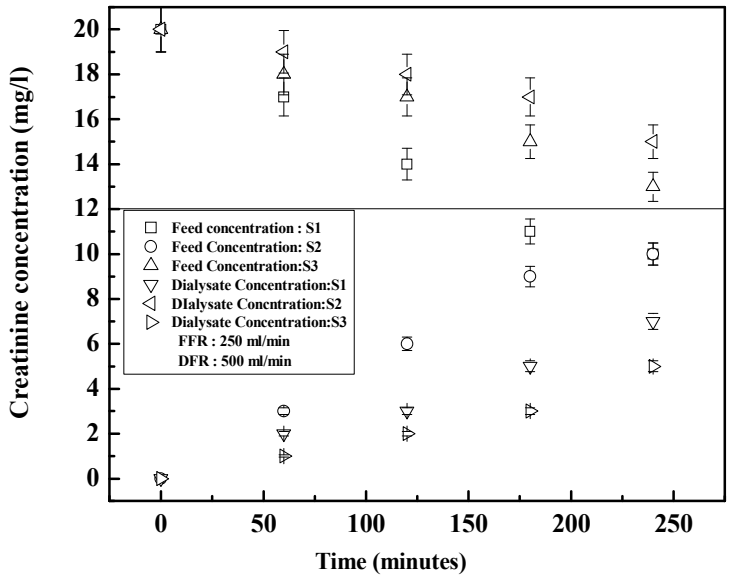

(b)

Fig. 14: Uremic toxin transport through three membranes: (a) Urea transport, (b) Creatinine transport.

3.5 Comparison with state of the art literature

Table 1 and 2 illustrate a detailed comparison between the present work and recent reported literature. It is evident from Table 1 that detailed membrane characterization has been carried out in the present work. Hydraulic permeability, MWCO and surface hydrophilicity have been investigated and the reported values are comparable with the literature data. However, mechanical strength, porosity as well as surface charge are few of additional aspects that have been quantified in the present work. The important interplay of these characteristics with biocompatibility has already been discussed in earlier sections. Table 2 presents a detailed comparison of the present work in terms of cytocompatibility and hemocompatibility with available literature. Two important aspects are evident from this information. First, exhaustive cytocompatibility and hemocompatibility tests have been

RSC Advances Accepted Manuscript

carried out in this work totalling 9 parameters as described in Table 2. Second, the developed materials in the present work show competitive results with the reported literature.

Table 1 : Comparison of membrane physiological properties with state of art literature

Membrane Properties	**Present Work**	**State of art literature**[15-20, 36]
Hydraulic permeability (m/s.Pa)	$0.2-1.4\times10^{-10}$	$3.12\times10^{-11}-4.16\times10^{-10}$
Molecular weight cut off (kDa)	6	--
Contact Angle	68^0-80^0	56^0-72^0
Tensile strength (MPa)	6-11	--
Porosity (%)	53-62	--
Surface charge (mV)	-0.03-0.1	--
Surface morphology (SEM)	Studied	Studied

RSC Advances Accepted Manuscript

Table 2 : Comparison of membrane cytocompatibility and hemocompatibility with state of art literature

	Present Work	**State of art literature**					
		Li et al.[15]	Nie et al.[16]	Higuchi et al.[17]	Dahe et al.[18]	Shakaib et al.[19,20]	Lin et al.[36]
Material	PSf-PVP-PEG; Surface modified PSf ; PAN homopolymer.	PES blended with citric acid grafted polyurethane	Carbon nanotube grafted PES composite.	Chemically modified PSf.	PSf-vitamin E-TPGS composite.	Blend polyamide and monosodium glutamate blend.	PAN immobilized with chitosan and heparin.
Cytocompatibility							
Metabolic activity (% better than control)	√√ (37%)	√√ (24%)	√√ (30%)	--	√√ (33%)	--	
Cell proliferation	√√	--	--	--	√√	--	--
Oxidative stress	√√	--	--	--	√√	--	--
Total protein adsorption ($\mu g/cm^2$)	√√ 15-30	√√ 18-34	√√ 7-15	√√ 3-8	√√ 18-30	--	--
Cell attachment and morphology (SEM and confocal imaging)	√√	--	--	--	√√	--	--
Hemocompatibility							
Hemolysis	√√	--	--	--	√√	--	--
Blood cell aggregation	√√	--	--	--	--	--	--
Platelet adhesion	√√	√√	√√	√√	√√	--	--
Thrombus formation	√√	--	--	--	√√	--	--

RSC Advances Accepted Manuscript

4.0 Conclusion

(i) Three types of dialysis grade membrane of identical MWCO was synthesized and characterized in detail. The permeability, mechanical strength, contact angle, surface charge, porosity and membrane morphology was analyzed. It was found that S1 (PSf-PVP-PEG) blend membrane had the highest permeability (1.2×10^{-10} m/Pa.s), least contact angle (69 º) and highest porosity (62 %). The surface charge of the membrane was found to near neutral.

(ii) The biological assessment of the three membranes were carried out comprehensively. It was found that S1, S2 and S3 were cytocompatible, displaying promising proliferation, metabolic activity as well as minimum cell adhesion and ROS activity.

(iii) The hemocompatibility performance of synthesized membranes were comparable. The blood cells aggregation activity was similar in all three membranes. Interestingly, the prepared membrane exhibited very low hemolysis activity compared to control. Further, a varying trend of platelet adhesion was found among three membranes owing to their protein adhesion nature. S1 adhered less platelets compared to S2 and S3, which followed in thrombus formation activity. Overall S1 and S2 have comparable and are better in hemocompatibility than S3 and commercial membrane.

(iv) The transport of uremic toxins indicated that S1 and S2 facilitated the permeation than S3. While it took only 120 minutes for S1 and S2 to bring down the urea concentration from 500 to less than 400 mg/l, the same for S3 was 180 minutes. Similar results were obtained for creatinine transport as well.

5.0 Acknowledgment

RSC Advances Accepted Manuscript

This work is partially supported by a grant from the Department of Science and Technology, Government of India, and Forus under the scheme no. IDP/MED/7/2011, dt. 05.03.2012 . Any opinions, findings and conclusions expressed in this paper are those of the authors and do not necessarily reflect the views of DST.

References:

1. The Renal Association, Normal GFR, 2013, http://www.renal.org/information-resources/the-uk-eckd-guide/normal-gfr#sthash.Qoxv8mmG.dpbs

2. W. J. Kolff and H. T. J. Berk, *Acta. Med. Scand.,* 1944**, 117**, 121-134.

3. N. Alwall, *Copenhagen, Munksgaard,* 1963.

4. T. Graham, *Phil. Trans. Roy. Soc. London,* 1854**, 144**,177-228.

5. A. Fick, *Annual Physik. Chem.*,1855, **94**, 59-86.

6. W. R.Clark, R. J. Hamburger and M. J. Lysaght, *Kidney Int*., 1999, 56, 2005-2015.

7. T. Kinoshita, *Immunol. Today.,* 1991, **12**, 291-294.

8. S. Bowry and T. Rintellen *ASAIO J*., 1998, **44**, 579-583.

9. M.C. Yang and W.C. Lin, *J. Polym. Res.*, 2002*,* **9**, 201–206.

10. H.G. Hicke, P. Bohme, M. Becker, H. Schulze and M. Ulbricht, *J. Appl. Polym. Sci.*, 1996, **80**, 1147–1161.

11. M. Ulbricht and A. Papra, *Enzyme Microb. Technol.*, 1997, **20**, 61–68.

12. M. Ulbricht and G. Belfort, *J. Membr. Sci.*, 1996, **111**, 193–215.

13. M. Hayama, T. Miyasaki, S. Mochizuki, H. Asahara, K. Tsujioka, F. Kohori, K. Sakai, Y. Jinbo, and M. Yoshida, *J. Membr. Sci.*, 2002, **210**, 45-53.

RSC Advances Accepted Manuscript

14. A.C. Yamashita *Contrib Nephrol.* Basel, Karger, 2011, **173**, 58–69.

15. L . Li, C. Cheng, T.Xiang, M. Tang, W. Zhao, S. Shun and C. Zhao, *J. Membr. Sci.*, 2012, **405-406**, 261-274.

16. C. Nie, L. Ma, Y. Xia, C. He, J. Deng, L. Wang, C. Cheng, S. Sun and C. Zhao, *J. Membr. Sci.*, 2015, **475**, 455-468.

17. A. Higuchi, K. Shirano, M. Harashima, B. O. Yoon, M. Hara, M. Hattori and K. Imamura, *Biomaterials*, 2002, **23**, 2659-2666.

18. G. J. Dahe, R. S. Teotia, S. S. Kadam and J. Bellare, *Biomaterials*, 2011, **32**, 352-365.

19. M. Shakaib, I. Ahmed, R. M. Yunus and A. Idris*, Int. J. Polym. Mater. Polym. Biomat.*, 2013, **62**, 345-350.

20. M. Shakaib, I. Ahmed, R. M. Yunus and M. Z. Noor*, Int. J. Polym. Mater. Polym. Biomat.*, 2014, **63**, 80-85.

21. A. Saito, *Contrib Nephrol.* Basel, Karger, 2011, **173**, 1-10.

22. S. K. Bowry, E. Gatti and J. Vienken, *Contrib Nephrol.* Basel, Karger, 2011, **173**, 110-118.

23. A.M. MacLeod, M.K. Campbell, J.D. Cody, C. Daly, A. Grant, I. Khan, K.S. Rabindranath, L. Vale and S.A. Wallace, *Cochrane Database Syst Rev.*, 2005, Issue 3. Art. No.: CD003234

24. S.K. Bowry, *Inter. J. Artif. Organs,* 2002*,* **25**, 447-460.

25. S. Qiu, L. Wu, L. Zhang, H. Chen and C. Gao, *J. Appl. Pol. Sci.,* 2009, **112**, 2066-2072.

RSC Advances Accepted Manuscript

26. A. Roy and S. De, *J. Food. Eng.,* 2014, **126**, 7–16.

27. P. Rai, G. C. Majumdar, S. Dasgupta and S. De, *LWT – Food Sci. Technol.,* 2007, **40**, 1765-1773.

28. S. Banerjee and S.De, *J. Membr. Sci.,* 2012, **389**, 188-196.

29. J. F. Li, Z. L. Xu, H. Yang, L. Y. Yu and M. Liu, *Appl. Surf. Sci.,* 2009, **255**, 4725-4732.

30. S. R. Panda and S. De, *J. Pol. Res.,* 2013, **20**, 179-195.

31. S. Chatterjee and S. De, *Sep. Purif. Technol.,* 2014; **125**, 223-238.

32. T. Mosmann, *J. Immunol. Methods*., 1983, **65**, 55-63.

33. B. Das, P. Dadhich, P. Pal, P. K. Srivas, K. Bankoti and S. Dhara, *J. Mater. Chem. B,* 2014, ***2*(39)**, 6839–6847.

34. P. K. Smith, R. I. Krohn, G. T. Hermanson, A. K. Mallia, F. H. Gartner, M D. Provenzano, E. K. Fujimoto, N. M. Goeke, B. J. Olson and D. C. Klenk, *Anal. Biochem.,* 1985, **85**, 76–85.

35. F. Pati, P. Datta, B. Adhikari, S. Dhara, K. Ghosh, P. K. Das Mohapatra, *J. Biomed. Mater. Res. A,* 2012, **100(4)**, 1068–79.

36. W. -C. Lin, T.-Y. Liu and M.-C. Yang, *Biomaterials*, 2004, **25**, 1947–1957.

37. W. Sun, J. Liu, H. Chu and B. Dong, *Membranes*, 2013, **3**, 226-241.

38. M. Hayama, K. Yamamoto, F. Kohori and K. Sakai, *J. Membr. Sci.*, 2004, **234**, 41-49.

39. M. Matsumoto, M. Yamaguchi, Y. Yoshida, M. Senuma, H. Takashima T. Kawamura and A. Hirose, *Food. Chem. Toxicol.*, 2013, **56**, 290–296.

40. Chemicalland21, 2012. N,N'-Diphenyl-p-Phenylenediamine. http://www.chemicalland21.com/

41. T. Satoh and M. Izumi, *Neurosci. Lett.*, 2007, **418(1)**, 102–105.

RSC Advances Accepted Manuscript

42. M. M. Santore and C. F. Wertz, *Langmuir*, 2005, **21**, 10172–10178.

43. K. Nakanishi, T. Sakiyama and K. Imamura, *J. Biosci. Bioeng.*, 2001, **91(3)**, 233–244.

44. T. Godjevargova and A. Dimov, *J. Membr. Sci.,* 1992, **67**, 283-287.

45. S. Y. Wong, L. Han, K. Timachova, J. Veselinovic and N. Hyder, *Biomacromolecules*, 2012, **13 (3)**, 719–726.

46. Z-G Wang, L-S Wan, and Z-K Xu, *J. Membr. Sci.*, 2007, **304**, 8–23.

47. C. R. Hasler, G. R. Owen, W. Brunner and W. H. Reinhart, *Nephrol. Dial. Transplant*, 1998, **13**, 3132-3137.

48. K. Ishihara, K. Fukumoto, Y. Iwasaki, and N. Nakabayashi, *Biomaterials*, 1999, **20**, 1553–1559.

49. M. Tanaka, T. Motomura, M. Kawada, T. Anzai, K. Yuu, T. Shiroya, K. Shimura, M. Onishi, and A. Mochizuki, *Biomaterials*, 2000, **21**, 1471-1481.

1

RSC Advances Accepted Manuscript